Multi-objective optimal reactive power dispatch to maximize power system social welfare in the presence of generalized unified power flow controller

Chintalapudi Venkata Suresh, Sirigiri Sivangaraju

Department of Electrical and Electronics Engineering
Jawaharlal Nehru Technological University Kakinada, Kakinada
Andhra Pradesh, 533 003, India
e-mail: venkatasuresh3@gmail.com

Abstract: In this paper a novel non-linear optimization problem is formulated to maximize the social welfare in restructured environment with generalized unified power flow controller (GUPFC). This paper presents a methodology to optimally allocate the reactive power by minimizing voltage deviation at load buses and total transmission power losses so as to maximize the social welfare. The conventional active power generation cost function is modified by combining costs of reactive power generated by the generators, shunt capacitors and total power losses to it. The formulated objectives are optimized individually and simultaneously as multi-objective optimization problem, while satisfying equality, in-equality, practical and device operational constraints. A new optimization method, based on two stage initialization and random distribution processes is proposed to test the effectiveness of the proposed approach on IEEE-30 bus system, and the detailed analysis is carried out.

Key words: generalized unified power flow controller, optimal reactive power dispatch, social welfare, multi-objective optimization

1. Introduction

The conventional regulated power system is becoming modern deregulated power system by providing open-access and competitive environment. At present, the power system is operating at its maximum limit to satisfy the basic requirements of demand. But the economic concerns are considered for active power generation only. In practice, it is necessary to generate reactive power in an optimal way, to minimize the deviation of voltage at load buses so as to minimize the total power losses in a given system. The reactive power plays an important role to avoid the system from voltage collapse.

To increase the effectiveness of the market structure, it is necessary to consider the payment for reactive power produced by synchronous generator and capacitors [1-3]. Lack of reactive power, increases the voltage drop at some buses and leads to system voltage instability [4]. In [5] the power market clearing using multi-objective optimization is proposed. NERC-10 clearly reveals that, the reactive power can be considered for financial compensation [6]. A method to calculate both real and reactive power spot prices of selected ancillary services has been developed in [7].

The role of FACTS device in open power market is to manage the congestion, enhancing security and available capability, controlled power flow, and to improve system performance [8]. A method to identify suitable location to install UPFC to meet different objectives is proposed in [9-10]. The effect of reactive power marginal cost on social welfare was proposed in [11]. Detailed cost models of reactive power and its effect in deregulated environment are proposed in [12, 13]. Optimal reactive power dispatch into different nodal pricing algorithms are presented in [14, 15]. Multi-objective based optimal reactive power dispatch problem was solved using evolutionary algorithms is presented in [16-19].

From the careful review of the literature, it is identified that, most of them are concentrated on either optimal reactive power dispatch problem or social welfare maximization problem. In practical power system, the independent system operator always tries to maximize the social welfare through optimal reactive power dispatch. Hence it is necessary to study the effectiveness of the problem using multi-objective optimization problem. Further the available literature concentrated on single line power flow controllers, but it is confirmed that, multi-line power flow controllers are more effective than the single line controllers. Consolidating all the above issues, in this paper, the main contribution is to enhance the system social welfare in the presence of one of the advanced FACTs multi-line convertible static controller formerly known as Generalized Unified Power Flow Controller (GUPFC). The following objectives are formulated for the proposed problem:

- Minimization of voltage deviation at load buses.
- Minimization of total transmission power loss.
- Maximization of social welfare.

The proposed Optimal Power Flow (OPF) problem is optimized by considering above objectives individually as well as simultaneously while satisfying equality, in-equality, practical and device limits. A methodology based on two-stage initialization along with uniform distributions of control parameters is proposed to enhance the optimization technique performance. The more realistic multi-fuel active and reactive power costs are formulated along with the costs of reactive power generated by the shunt capacitors and total power losses. The complete power injection model of GUPFC along with respective power injections is given to analyze the stated hypothesis. It is most significant to identify the proper location to install GUPFC in a given system to enhance the system security and the complete methodology is described with supporting results. The effectiveness of the proposed method is tested on IEEE-30 bus test system.

2. Generalized unified power flow controller modelling

Normally GUPFC consist two/more series converters and one shunt converter. To show the effectiveness of the control operation of GUPFC, two series converters are coordinated with one shunt converter is shown in Figure 1.
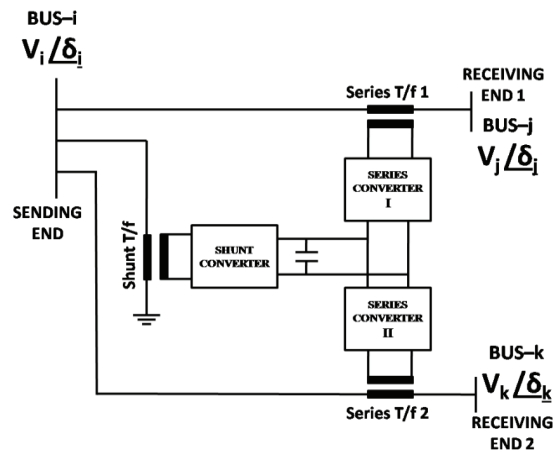

Fig. 1. Basic configuration of two series converter GUPFC

In this paper, the following rules are considered, to identify the proper device location so as to reduce the number of possible locations.
- It should be located between two PQ buses and there should not be any shunt capacitors.
- It should not be placed in a line where tap changing transformer exists.

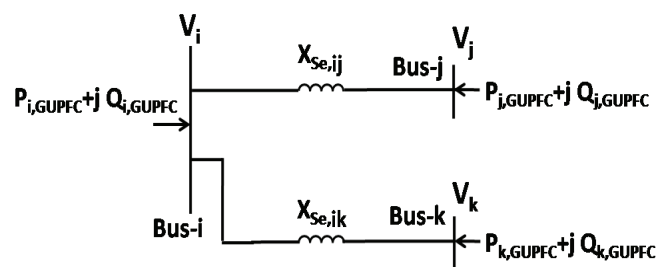The final steady state power injection model of GUPFC is shown in Figure 2.

Fig. 2. Injection model of two series converter GUPFC

The injected active and reactive powers can be expressed as

$$P_{i,GUPFC} = -V_i^2 \left[\sum_{q=j,k} r_{iq} B_{se,iq} \sin \gamma_{iq} \right] - 1.03 \left(\sum_{q=j,k} r_{iq} V_i V_q B_{se,iq} \sin(\delta_{iq} + \gamma_{iq}) - r_{iq} V_i^2 B_{se,iq} \sin \gamma \right), \quad (1)$$

www.czasopisma.pan.pl   PAN   www.journals.pan.pl   POLSKA AKADEMIA NAUK

408   C. Venkata Suresh, S. Sivangaraju   Arch. Elect. Eng.

$$Q_{i,GUPFC} = -V_i^2 \left[\sum_{q=j,k} r_{iq} B_{se,iq} \cos\gamma_{iq} \right] + Q_{sh},$$ (2)

$$P_{p,GUPFC} = r_{ip} V_i V_p B_{se,ip} \sin(\delta_{ip} + \gamma_{ip}) \quad \forall \quad p = j,k,$$ (3)

$$Q_{p,GUPFC} = r_{ip} V_i V_p B_{se,ip} \cos(\delta_{ip} + \gamma_{ip}) \quad \forall \quad p = j,k.$$ (4)

The coefficient 1.03 represents the converter switching loss factor, where r and γ are respective per unit magnitude and phase angles of the series voltage sources operating within the limits $0 \leq r \leq r\max$ and $0 \leq \gamma \leq \gamma\max$. '$B_{se} = 1/X_{se}$' is the susceptance of the series converter transformers.

2.1. Power mismatch equations

The power mismatch equations in Newton Raphson (NR) method can be modified by using the following equations.

$$\Delta P_{i,new} = \Delta P_{i,old} + P_{i,GUPFC},$$ (5)

$$\Delta Q_{i,new} = \Delta Q_{i,old} + Q_{i,GUPFC},$$ (6)

where, $\Delta P_{i,old}$ and $\Delta Q_{i,old}$ are the power mismatches without device. Similar modifications can be obtained for the remaining GUPFC buses.

2.2. Jacobian elements

The Jacobian elements can be modified in the NR iterative process using the following equations

$$\left(H^{new} = H^{old} + H' \right).$$

$$H'_{ii} = \frac{\partial P_{i,GUPFC}}{\partial \delta_i} = -1.03 \left[\sum_{q=j,k} r_{iq} V_i V_q B_{se,iq} \cos(\delta_{iq} + \gamma_{iq}) \right],$$ (7)

$$H'_{qq} = -r_{iq} V_i V_q B_{se,iq} \cos(\delta_{iq} + \gamma_{iq}) = -Q_{q,GUPFC} \quad \forall \quad q = j,k,$$ (8)

$$H'_{iq} = 1.04 [r_{iq} V_i V_q B_{se,iq} \cos(\delta_{iq} + \gamma_{iq})] = 1.04 Q_{q,GUPFC} \quad \forall \quad q = j,k,$$ (9)

$$H'_{qi} = r_{iq} V_i V_q B_{se,iq} \cos(\delta_{iq} + \gamma_{iq}) = Q_{q,GUPFC} \quad \forall \quad q = j,k,$$ (10)

where H^{old} is the Jacobian element without device. Similar modifications can be obtained for the remaining elements.

2.3. Investment cost

Conventionally, UPFC can be considered as a combination of STATCOM and SSSC. Similarly, GUPFC gives the combined effect of UPFC and SSSC. Hence, the investment cost of GUPFC can be considered as the sum of investment costs of UPFC and SSSC.

$$ICGUPFC, i\text{-}j\text{-}k = ICUPFC, i\text{-}j + ICSSSC, i\text{-}k$$ (11)

Investment cost of UPFC [20] over a period of 15 years can be given as

$$IC_{UPFC} = \frac{C_{UPFC} \times S_{UPFC} \times 1000}{15 \times 8760} \qquad \$/h. \tag{12}$$

Here, Cost of Installation of UPFC is

$$C_{UPFC} = 0.0003\,S_{UPFC}^2 - 0.2691\,S_{UPFC} + 188.22 \qquad \$/kVAr. \tag{13}$$

Operating range of UPFC(S_{UPFC}) in MVAr is $S_{UPFC} = |Q_2| - |Q_1|$, where Q_1, Q_2 are the reactive power flows in the line before and after placing UPFC. Similarly, the Investment Cost (IC) of SSSC [21] is

$$IC_{SSSC} = \frac{S_{SSSC} \times \eta \times CRF}{n \times 8760}\,\$/h, \tag{14}$$

where

$$CRF = \text{Capital recovery factor} = \frac{l(1+l)^n}{(1+l)^n - 1},$$

'l' is discount rate (6%), 'n' is life time (15 years) of SSSC, and 'η' is the investment cost co-efficient (50,000 \$/MVA).

2.4. Incorporation procedure

The overall computational procedure of Newton-Raphson power flow method with device can be described in the following steps.

Step 1. Read bus data, line data and GUPFC data.

Step 2. Assume flat voltage profile and set iteration count $k = 0$.

Step 3. Compute active and reactive power mismatch from the scheduled and calculated powers and also GUPFC power injections using Equations (1-4).

Step 4. Determine Jacobian matrix using power flow equations.

Step 5. Modify power mismatch and Jacobian with respective device elements to Incorporate GUPFC in load flow using Equations (5-10).

Step 6. Solve the NR method equations to find the voltage magnitude and angles correction vector.

Step 7. Update the solution using correction vector.

Step 8. Increase the iteration count, $k = k + 1$ and repeat steps from 5 to 7.

Step 9. Stop the process, if the maximum mismatch is less than given tolerance.

3. Optimal location

The device installation location will enhance the system security either by minimizing line loadings or bus voltage limit violations under contingency operations. Here the system severity function (F_{severity}) can be expressed as [22]

www.czasopisma.pan.pl PAN www.journals.pan.pl POLSKA AKADEMIA NAUK

410 C. Venkata Suresh, S. Sivangaraju Arch. Elect. Eng.

$$F_{\text{severity}} = \sum_{i=1}^{N_{\text{line}}} \left(\frac{S_i}{S_i^{\max}} \right)^{2q} + \sum_{j=1}^{N_{\text{bus}}} \left(\frac{V_{j,ref} - V_j}{V_{j,ref}} \right)^{2r}, \tag{15}$$

where N_{line}, N_{bus} are the total number of lines and buses in a given system. S_i and $S_i^{\max}$ are the present and maximum apparent powers of ith line. $V_{j,ref}$ and V_j are the nominal voltage and present voltage values at jth bus. 'q' and 'r' are two coefficients used to penalize more or less over loads and voltage violations. These are considered to be equal to 2.

To enhance security of the system under contingencies, GUPFC should be placed in a proper location. Initially contingency analysis is performed by removing single transmission line at a time and identifies total Number of Voltage Violation Buses (NVVB) and total Number of Over Loaded Lines (NOLL). Calculate performance index by adding NVVB and NOLL. Finally the contingency with highest performance index value is identified as most critical one.

Then, this critical line is removed from the system and GUPFC is placed in one of the possible installation locations discussed in section-II, and the severity function (Fseverity) is minimized subjected to satisfy equality, in-equality, practical constraints and device control settings. This process is repeated at all possible installation locations, and finally, identifies the location for placing device which has less severity value for enhancing the system security.

4. Multi-Objective problem formulation

Many of the optimization problems discussed in the literature is restricted to either of the certain objectives like Generation Cost, power loss and voltage deviations. But in practice it is necessary to optimize these objectives simultaneously by satisfying equality, inequality, practical and device constraints. Hence, it is clear that the effectiveness and efficiency of multi-objective algorithm gives best compromised solution by satisfying constraints on a system.

Aggregating all objectives and constraints, the problem can be formulated mathematically as a constrained nonlinear multi-objective optimization problem as follows:

$$\text{Min} / \text{Max} \ \left[A_m(x, u) \right]; \quad \forall m = 1, 2, ..., J. \tag{16}$$

Subjected to $g(x, u) = 0$; $h(x, u) \leq 0$, where 'g' and 'h' are the equality and inequality constraints respectively and 'x' is a control vector of dependent variables like slack bus active power generation $(P_{g,\text{slack}})$, load bus voltage magnitudes (V_L) and generator reactive powers (Q_G) and vector 'u' consist control variables such as active powers (P_G) and voltages (V_G) of generators, transformer tap ratios (T) and shunt compensation (Q_{Sh}) and device control parameters. 'J' is the total number of objective functions.

Multi-Objective optimization can have two or more objective functions to be optimized at a time. As a result, there is no unique solution to multi-objective optimization problems, but the aim is to find all possible compromised solutions available in search space (called Pareto front set). The considered objectives are formulated as follows.

4.1. Voltage deviation

The voltage deviation at load buses needs to be minimized to optimize the reactive power dispatch problem and can be expressed as

$$A_1 = Vdev = \sum_{i=1}^{N_{load}} \left| V_i - V_i^{spe} \right|, \tag{17}$$

where, V_i is the voltage at load bus-i, V_i^{spe} is the voltage set to be '*1* p.u.' and N_{load} is the number of load buses.

4.2. Total power loss

In power system, the active power loss should be minimized to enhance power delivery performance and can be calculated using

$$A_2 = TPL = \sum_{i=1}^{N_{line}} g_i \left[V_i^2 + V_j^2 - 2V_iV_j \cos(\delta_i - \delta_j) \right] \quad MW, \tag{18}$$

where g_i is the conductance of ith line which connects buses *i* and *j*. V_i, V_j and δ_i, δ_j are voltage magnitude and angle of ith and jth buses.

4.3. Social welfare

While clearing the market price, the cost for the power consumed by the load should be considered. Conventionally, social welfare includes the costs of active power generations and its corresponding loads. This conventional problem is modified by combining costs of reactive power generated by the generators, shunt compensators, and total transmission losses in addition to the cost of active power generated by the generators. This function can be formulated as

$$A_3 = SW =$$

$$= \max \left[\sum_{i=1}^{N_D} B_{Di}(P_{Di}) - \left(\sum_{i=1}^{N_G} C_{Gi}(P_{Gi}) + \sum_{i=1}^{N_G} C_{Gi}(Q_{Gi}) + \sum_{i=1}^{N_{sh}} C_{Shi}(Q_{Shi}) + C(TPL) + IC_{GUPFC} \right) \right]. \tag{19}$$

The demand side cost function $B_{Di}(P_{Di})$ can be expressed as

$$B_{Di}(P_{Di}) = -a_{id}P_{Di}^2 - b_{id}P_{Di} + c_{id} \qquad \$/h, \tag{20}$$

where, ND is the total number of demands in the system, a_{id}, b_{id}, c_{id} are demand side bidding coefficients. Similarly the remaining sub functions are formulated as follows,

4.3.1. Multi-fuel non-convex cost of active power

In practical, generating stations are supplied with different types of fuels like coal, fossil fuel, oil and gas etc to generate electrical power. The formulated multi-fuel active power cost function can be expressed as

$$\sum_{i=1}^{N_G} C_{Gi}(P_{Gi}) = \left(\sum_{i=1}^{2} F_i(P_i)\right) + \left(\sum_{i=3}^{N_G} F_i(P_i)\right), \tag{21}$$

$$F_i(P_i) = \begin{cases} a_{i1}P_i^2 + b_{i1}P_i + c_{i1} + \left|e_{i1} \times \sin\left(f_{i1} \times \left(P_i^{\min} - P_i\right)\right)\right| & ; \quad P_i^{\min} \le P_i \le P_i^1 \\ a_{i2}P_i^2 + b_{i2}P_i + c_{i2} + \left|e_{i2} \times \sin\left(f_{i2} \times \left(P_i^{\min} - P_i\right)\right)\right| & ; \quad P_i^1 \le P_i \le P_i^2 \\ \dots \\ a_{ik}P_i^2 + b_{ik}P_i + c_{ik} + \left|e_{ik} \times \sin\left(f_{ik} \times \left(P_i^{\min} - P_i\right)\right)\right| & ; \quad P_i^{k-1} \le P_i \le P_i^{\max} \end{cases},$$

where $a_{ik}, b_{ik}, c_{ik}, e_{ik}, f_{ik}$ are the active power cost-coefficients of the ith unit with valve-point effects for fuel type k. The cost coefficients for the generators of the test system are given in Table A1.

4.3.2. Multi-fuel non-convex cost of reactive power

Careful study of literature reveals that, the generators active and reactive cost curves has similar characteristics. However, the cost of reactive power is less compared to that of active power. A new objective function for multi-fuel non convex reactive power cost can be expressed as

$$\sum_{i=1}^{N_G} C_{Gi}(Q_{Gi}) = \left(\sum_{i=1}^{2} F_i(Q_i)\right) + \left(\sum_{i=3}^{N_G} F_i(Q_i)\right), \tag{22}$$

$$F_i(Q_i) = \begin{cases} a_{ir1}Q_i^2 + b_{ir1}Q_i + c_{ir1} + \left|e_{ir1} \times \sin\left(f_{ir1} \times \left(Q_i^{\min} - Q_i\right)\right)\right| & ; \quad Q_i^{\min} \le Q_i \le Q_i^1 \\ a_{ir2}Q_i^2 + b_{ir2}Q_i + c_{ir2} + \left|e_{ir2} \times \sin\left(f_{ir2} \times \left(Q_i^{\min} - Q_i\right)\right)\right| & ; \quad Q_i^1 \le Q_i \le Q_i^2 \\ \dots \\ a_{irk}Q_i^2 + b_{irk}Q_i + c_{irk} + \left|e_{irk} \times \sin\left(f_{irk} \times \left(Q_i^{\min} - Q_i\right)\right)\right| & ; \quad Q_i^{k-1} \le Q_i \le Q_i^{\max} \end{cases},$$

where $a_{irk}, b_{irk}, c_{irk}, e_{irk}, f_{irk}$ are the reactive power cost-coefficients of the ith unit with valve-point effects for fuel type k. The reactive cost coefficients for the generators of the test system are given in Table A2.

4.3.3. Cost of capacitor's reactive power

The reactive power injected by the shunt capacitors affects the bus voltage at which it is connected. The cost of the reactive power should be calculated based on capital investment cost [23, 24] only.

$$C_{Shi}(Q_{Shi}) = \frac{Investment \; \cos t \times Q_{Shi}}{Operating \; hours}. \tag{23}$$

4.3.4. Cost of total active power loss

The system voltage profile and system active power losses are affected by controlling reactive power flow through transmission lines. Generally, the system losses are compensated by slack generator. This cost can be expressed as [25]

$$C(TPL) = \lambda loss \times TPL, \tag{24}$$

where, $\lambda loss = 20$ \$/MW-h is the market energy clearing price.

4.4. Constraints

The above problem is optimized by satisfying the following equality, in-equality, practical and also device limits.

4.4.1. Equality Constraints

These constraints are typically load flow equations.

$$\sum_{i=1}^{N_G} P_{G_i} - P_D - P_L = 0; \quad \sum_{i=1}^{N_G} Q_{G_i} + Q_{sh} - Q_D - Q_L = 0.$$

4.4.2. In-equality Constraints

Generator bus voltage limits: $V_{G_i}^{\min} \le V_{G_i} \le V_{G_i}^{\max}$; $\quad \forall i \in N_G$.

Active Power Generation limits: $P_{G_i}^{\min} \le P_{G_i} \le P_{G_i}^{\max}$; $\quad \forall i \in N_G$.

Transformers tap setting limits: $T_i^{\min} \le T_i \le T_i^{\max}$; $\quad i = 1,2,...,n_t$.

Capacitor reactive power generation limits: $Q_{Sh_i}^{\min} \le Q_{Sh_i} \le Q_{Sh_i}^{\max}$; $\quad i = 1,2,....,n_C$.

Transmission line flow limit: $S_{l_i} \le S_{l_i}^{\max}$; $\quad i = 1,2,....,N_{line}$.

Reactive Power Generation limits: $Q_{G_i}^{\min} \le Q_{G_i} \le Q_{G_i}^{\max}$; $\quad \forall i \in N_G$.

Bus voltage magnitude limits: $V_i^{\min} \le V_i \le V_i^{\max}$ $\quad i = 1,2,....,N_{load}$, where n_t total number of taps, n_C total number of VAr sources, N_{load} total number of VAr sources.

The above mentioned problem can be generalized using penalty factors as follows:

$$A_{m,aug}(x,u) = A_m(x,u) + R_1\left(P_{g,slack} - P_{g,slack}^{\lim}\right)^2 + R_2 \sum_{i=1}^{N_{Load}}\left(V_i - V_i^{\lim}\right)^2 + R_3 \sum_{i=1}^{N_G}\left(Q_{G_i} - Q_{G_i}^{\lim}\right)^2$$
$$+ R_4 \sum_{i=1}^{N_{line}}\left(S_{l_i} - S_{l_i}^{\max}\right)^2,$$

where R_1, R_2, R_3 and R_4 are the penalty quotients having large positive value. The limit values are defined as

$$x^{\lim} = \begin{cases} x^{\max}, & x > x^{\max} \\ x^{\min}, & x < x^{\min} \end{cases}.$$

Here x is the value of $P_{g,slack}, V_i$ and Q_{G_i}.

4.5. Practical constraints

Prohibited Operating Zones (POZ)

In practice when adjusting the output of a generator unit one must avoid the operation in the prohibited zones to increase the performance of a thermal unit during vibrations in the shaft or other machine faults. This feature can be included in the Non-convex economic dispatch problem formulation as follows:

$$P_i = \begin{cases} P_i^{\min} \leq P_i \leq P_{i,1}^L \\ P_{i,k-1}^U \leq P_i \leq P_{i,k}^L \quad k = 2,3,...,n_i, \\ P_{i,n_i}^U \leq P_i \leq P_i^{\max} \end{cases}$$

where n_i is the number of prohibited zones and k index of prohibited zone of unit-*i*. $P_{i,k}^L$ and $P_{i,k}^U$ are the respective lower and upper limit of kth prohibited zone of ith generator.

Ramp-rate constraints

The operating range of the generating units is restricted by their ramp rate limits to operate generators continuously between two adjacent periods forcibly. The inequality constraints due to ramp limits are

$$\max\left(P_{G_i}^{\min}, P_i^0 - DR_i\right) \leq P_{G_i} \leq \min\left(P_{G_i}^{\max}, P_i^0 + UR_i\right),$$

where P_i^0 is the power generation of ith unit at previous hour. DR_i and UR_i are the respective decreasing and increasing ramp-rate limits of ith unit.

4.6. Device limits

The following limits are considered for GUPFC.

$$r_{iq}^{\min} < r_{iq} < r_{iq}^{\max} \quad ; \quad \forall \quad q = j,k ,$$

$$\gamma_{iq}^{\min} < \gamma_{iq} < \gamma_{iq}^{\max} \quad ; \quad \forall \quad q = j,k ,$$

$$B_{se,iq}^{\min} < B_{se,iq} < B_{se,iq}^{\max} \quad ; \quad \forall \quad q = j,k .$$

5. Uniformly distributed two-stage particle swarm optimization

Many programming languages used for simulation of applications needs to generate pseudo random numbers, which are effectively distributed using standard uniform distributions. Uniform distribution is one of the important members in the family of symmetric probability distribution. In this, all distributions have equal probability intervals. This is used to generate random variables between limits 'a' and 'b'. This distribution can be abbreviated as U(a, b) [47].

5.1. Initialization

Start the process by setting iteration is equal to zero. In this method, generate control variables uniformly rather than randomly as in existing PSO, between its minimum and maximum limits. In MATLAB environment, we have a flexibility to generate control variables using the following expressions

Existing PSO: a + (b-a)*rand(population number, particles number)

Proposed UDTPSO: random('unif', a, b, population number, particles number)

While in other programming languages, the variables can be generated uniformly by following the uniform distribution procedure given in [48].

5.2. Two stage initialization

The first stage of the process is that, update the system data with newly generated control variables and evaluate the objective function and fitness values. The second stage of the process is that, obtaining the pair wise best population using comparison process between previously obtained solutions. The final solutions are treated as local best values. From these solutions, identify global best value. Start the iterative process by calculating dynamic weight and new velocities and update the position of the particles. The chaotic inertia weight [24, 29] is calculated based on the experience of the previous positions and velocities of the particles. Because of this, the iterative process starts with large inertial weight to search global best values and decreases its value as iterations increases to benefit the local best values. Evaluate the function using new position of the particles and update global and local best values. The complete methodology is shown in Figure 3.
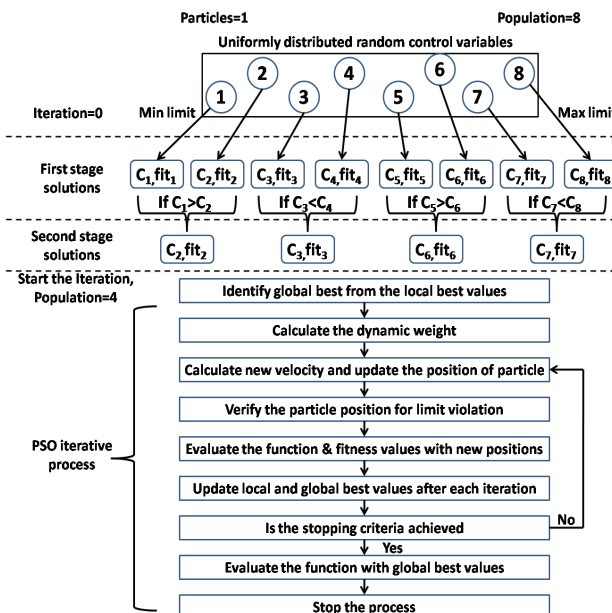

Fig. 3. Methodology of the proposed UDTPSO

5.3. Fuzzy decision making tool

After solving total Pareto optimal solutions (M) for a given optimization sub problems using Non-dominated sorting UDTPSO, the best compromised optimal settings are chosen by the decision maker. For this purpose, fuzzy decision making tool calculate a linear membership function (μ_m) for minimization of objective functions [29, 30] is

$$\mu_m^n = \begin{cases} 1 & ; & A_m^n \leq \min(A_m) \\ \dfrac{\max(A_m) - A_m^n}{\max(A_m) - \min(A_m)}; & \min(A_m) \leq A_m^n \leq \max(A_m) \\ 0 & ; & A_m^n \geq \max(A_m) \end{cases} \tag{25}$$

for maximization of objective functions is

$$\mu_m^n = \begin{cases} 0 & ; & A_m^n \leq \min(A_m) \\ \dfrac{A_m^n - \min(A_m)}{\max(A_m) - \min(A_m)}; & \min(A_m) \leq A_m^n \leq \max(A_m), \\ 1 & ; & A_m^n \geq \max(A_m) \end{cases} \tag{26}$$

where, A_m^n and μ_m^n are the respective values of the ith objective function in the nth Pareto optimal solution and its membership function. The most preferred degree of the Pareto optimal solutions can be defined as

$$\mu_{opt} = \underbrace{\sup}_{n \in j} \dfrac{\displaystyle\sum_{i=1}^{p} W_i \mu_m^n}{\displaystyle\sum_{n=1}^{M} \sum_{i=1}^{p} W_i \mu_m^n}, \quad \text{where} \quad W_i \geq 0; \sum_{i=1}^{p} W_i = 1 \tag{27}$$

where W_i is the weight value of the ith objective function. Therefore, the best optimal Pareto solution and the corresponding settings are obtained by the proposed algorithm based on the adopted weight factors.

6. Implementation of proposed approach

The proposed NSUDTPSO algorithm to solve multi-objective problem is described in the following steps:

Step 1: Choose population size 'M' and generate the initial population for UDTPSO with in the control variable bounds, initialize the problem parameters (set iteration count = 0).

Step 2: For each of the individual, perform NR load flow with GUPFC described above using Eqns (1-10) and evaluate the objective function values using Equations (17-19).

Step 3: These solutions constituted as parent solutions.

Step 4: Each solution can be compared with the other solution in the population to find its dominance. Finally, identify different fronts 'Pf'.

Step 5: In order to find the individuals in the next nondominated front, the initial solutions are discounted temporarily and the above procedure is repeated during iteration process. The new solutions are called as off-spring solutions.

Step 6: Perform non-dominated sorting on the combined solutions (parent+off-spring) and identify different fronts 'Pf'.

Step 7: Crowding distance operation [31] is performed on the entire set of solutions in a Pareto front. This operation requires sorting the population according to each objective function value in ascending order of magnitude.

Step 8: The boundary values are assigned to an infinite distance value for each of the objective function. For the remaining population a distance value equal to the absolute normalized difference in the function values of two adjacent populations is assigned.

Step 9: This calculation is performed for all objectives and for all Pareto fronts.

Step 10: The sorting is performed on a given solutions according to their crowding distances, chose global best value among the top 10 solution in Pareto front and increase the iteration count.

Step 11: From Step 5 to Step.10 are repeated till maximum iterations reached.

Step 12: Then fuzzy membership values for non-dominated solutions in the Pareto-front are calculated using Equations 25-27 and the final solution have been chosen based on the operator's requirements.

7. Results and analysis

IEEE-30 bus system with 41 transmission lines is considered [32-35]. The total control variables in this system are 18, which include active power generation and voltage levels of 6 generators, 4 tap settings of tap-changing transformers and 2 shunt VAr sources.

To analyze the effect of GUPFC on defined objectives, each of the following cases are optimized without and with GUPFC and the corresponding results are tabulated.

Cases 1, 2 and 3 gives the results of voltage deviation (Vdev), total power loss (TPL) and social welfare (SW) objectives individually.

Case 4 analyzes the multi-objective optimization problem when two of the objectives considered together.

Case 5 optimizes the problem, when all three objectives are considered.

Initially, the formulated severity function given in Equation 15 is optimized. The optimal location to install GUPFC is identified by performing the procedure described in Section 4. The result of contingency analysis for this system is given in Table 1. To maintain the continuity either in supplying/receiving the power, the contingency analysis is not performed on lines between buses 9-11, 12-13, and 25-26. Hence, for this system only 38 transmission line contingencies out of 41 are considered. The result of only top 2 contingencies is tabulated.

From Table 3, it is very clear that, the line connected between buses 2 and 5 is the most critical one. By following the rules given in Section 2, there are 23 possible GUPFC installation locations.

www.czasopisma.pan.pl   www.journals.pan.pl

418   *C. Venkata Suresh, S. Sivangaraju*   Arch. Elect. Eng.

Table 1. Results of contingency ranking

S. No.	Line No	Outage line	Over loaded lines (Line flow/ MVA limit)	NOLL	Voltage Violated Buses	NVVB	PI	Rank
1	5	2-5	(1-2) (171.399/130) (2-4) (77.671/65) (2-6) (105.434/65) (4-6) (121.418/90) (5-7) (110.190/70) (6-8) (35.828/32)	6	–	0	6	1
2	36	28-27	(1-2) (180.949/130) (22-24) (20.246/16) 24-25) (19.501/16)	3	27 (0.8989) 29 (0.8760) 30 (0.8627)	3	6	2

Severity function is evaluated in all these locations with GUPFC and the top 5 least severity function valued locations are tabulated in Table.2 for rank-1 contingency.

Table 2. Severity function values for rank-1 contingency with GUPFC

Loc. No.	GUPFC location			Severity function value
	Sending end bus	Receiving end buses		
1	12	14	15	1517
2	12	14	16	1.6164
3	12	15	16	1.6492
4	15	12	23	1.6505
5	15	14	18	1.6668

From Table 2, it is observed that, first location is the best location for placing the GUPFC, because it has least severity function value. The further analysis is performed by placing device in this location.

The obtained results for cases 1, 2 and 3 are tabulated in Table 3. From this table it is observed that, while minimizing voltage deviation, the total power losses are increasing and vice-versa. In all these cases, it is proved that, with GUPFC the objective function values are improved. In case 1, 0.011 p.u voltage deviation is reduced with GUPFC, results 0.138 MW increase in TPL and 15.67 \$/h decrease in SW. Similarly, in case 2 with the decrease of 0.257 MW TPL results in decrease of SW by 94.083 \$/h and increase of Vdev by 0.043 p.u.. In case 3, as the SW is increased by 12.474 \$/h and consequently the TPL is decreased by 0.271 MW and Vdev is increased by 0.04 p.u..

The load cost in cases 1 and 2 is 1907.746 \$/h as the total active power demand on IEEE-30 bus system is 283.4 MW. In case 3, the total active power demand of 335.0607 MW is served without device and 327.9015 MW with GUPFC. Total generation cost includes the costs of active, reactive, shunt capacitor powers and transmission losses for without device and with device cost is given in Table 3. The convergence patterns for cases 1 and 2 are shown in Figures 3 and 4.

From Figures 3 and 4 it is observed that, with GUPFC the iterative process starts with good initial value and reaches final best value in less number of iterations when compared to without device, this is because of the effectiveness of the proposed method. The ramp rates and POZ limits followed by the generators is given in Table 4.
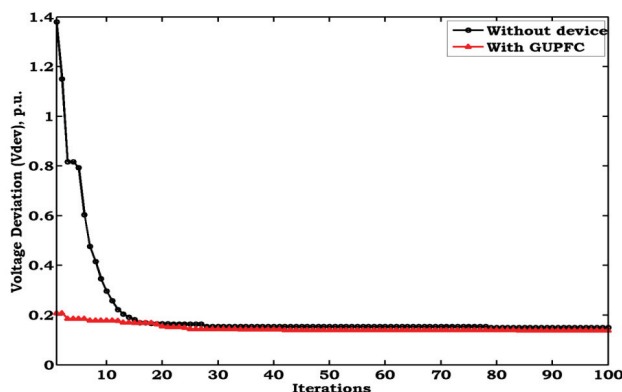

Fig. 3. Convergence characteristics of case-1 without and with GUPFC

Table 3. OPF results for cases 1, 2 and 3 without and with GUPFC

Control variables	Case 1		Case 2		Case 3		Minimum limit	Maximum limit
	Without	With	Without	With	Without	With		
PG1, MW	140.536	142.731	95.706	82.438	168.131	164.492	50	200
PG2, MW	44.585	42.626	49.985	63.000	50.000	50.000	20	80
PG5, MW	41.313	36.016	49.000	49.000	42.995	39.115	15	50
PG8, MW	24.178	23.456	30.000	30.000	24.914	25.000	10	35
PG11, MW	17.56	22.064	28.000	28.000	24.907	24.853	10	30
PG13, MW	22.439	23.865	35.000	35.000	33.773	33.857	12	40
VG1, p.u.	1.048	1.022	1.050	1.050	1.048	1.050	0.9	1.1
VG2, p.u.	0.977	0.990	0.995	1.012	0.952	1.034	0.9	1.1
VG5, p.u.	0.988	1.013	1.026	1.028	0.986	0.994	0.9	1.1
VG8, p.u.	1.022	1.005	1.031	1.031	0.986	0.999	0.9	1.1
VG11, p.u.	0.975	1.033	1.050	1.048	0.997	1.040	0.9	1.1
VG13, p.u.	0.962	1.010	1.050	1.050	1.012	0.998	0.9	1.1
Tap 6-9	0.980	1.052	1.045	0.992	0.991	1.023	0.9	1.1
Tap 6-10	1.068	0.963	0.952	1.027	1.048	0.978	0.9	1.1
Tap 4-12	0.921	0.969	1.000	1.006	1.005	0.990	0.9	1.1
Tap 28-27	0.961	0.955	0.974	0.980	1.025	0.987	0.9	1.1

|								
Qc 10, p.u.	29.959	22.948	21.618	20.031	18.190	25.613	5.0	30.0
Qc 24, p.u.	22.377	15.122	12.291	12.526	13.608	16.614	5.0	30.0
rij, p.u.	–	0.002	–	0.007	–	0.042	0.0	0.1
rik, p.u.	–	0.012	–	0.021	–	0.022	0.0	0.1
γij, deg.	–	133.027	–	114.406	–	158.066	0.0	360
γik, deg.	–	178.997	–	66.693	–	171.312	0.0	360
Xse,ij, p.u.	–	0.016	–	0.011	–	0.021	0.0	0.1
Xse,ik, p.u.	–	0.013	–	0.025	–	0.013	0.0	0.1
Qsh, p.u.	–	0.028	–	0.019	–	0.053	0.0	0.1
QG1, MVAr	39.359	−3.071	5.981	6.737	40.353	−2.484	−20	200
QG2, MVAr	−20.000	−20.000	−20.000	−20.000	−20.000	35.838	−20	100
QG5, MVAr	18.420	50.695	30.315	31.704	30.066	19.324	−15	80
QG8, MVAr	60.000	39.240	33.897	35.162	26.247	18.939	−15	60
QG11, MVAr	−10.000	16.998	14.268	8.065	6.213	15.242	−10	50
QG13, MVAr	−15.000	2.871	13.804	16.052	17.791	2.056	−15	60
Inv. COST, $/h	–	0.038	–	0.001	–	0.070	–	–
Vdev, p.u.	0.150	0.139	0.583	0.626	0.505	0.545	–	–
TPL, MW	7.211	7.349	4.291	4.037	9.660	9.389	–	–
Total gen cost, $/h	1001.971	1017.641	918.064	1012.663	1249.008	1197.229	–	–
Total load cost, $/h	1907.746	1907.746	1907.746	1907.746	2689.173	2649.868	–	–
SW, $/h	905.775	890.105	989.682	895.083	1440.165	1452.639	–	–
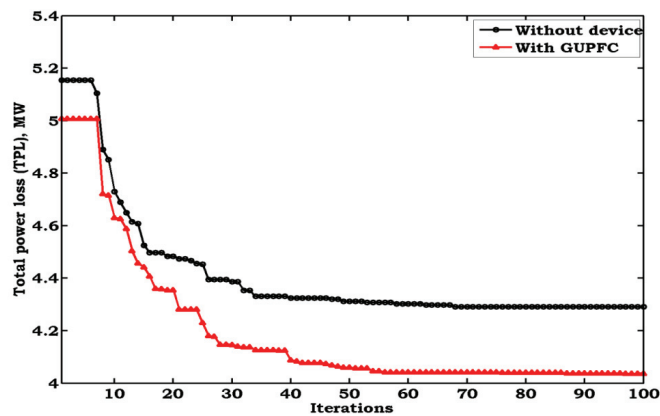
Fig. 4. Convergence characteristics of case-2 without and with GUPFC

From this table it is identified that, when maximizing social welfare, all generators are following up ramp-rates.

Table 4. Ramp rates and POZ limits followed by the generators for cases 1, 2, 3

Gen. No	Case 1		Case 2		Case 3	
	Without	With	Without	With	Without	With
1	Down, 2	Down, 2	Down, 1	Down, 1	Up, 2	Up, 2
2	Up, 1	Up, 1	Up, 1	Up, 2	Up, 3	Up, 3
5	Up, 2	Down, 2	Up, 2	Up, 2	Up, 2	Up, 2
8	Up, 1	Up, 1	Up, 4	Up, 4	Up, 1	Up, 3
11	Down, 1	Up, 1	Up, 4	Up, 4	Up, 1	Up, 1
13	Up, 1	Up, 1	Up, 2	Up, 2	Up, 2	Up, 2

1-Below POZ lower limit   2-Above POZ upper limit
3-Equal to POZ lower limit   4-Equal to POZ upper limit
UP-following up-ramp rate   Down-following down-ramp rate

In case 4, two of the objectives are considered to formulate multi-objective optimization problem. The results of this case are tabulated in Tables 5, 6 and 7.

Table 5. Summary of multi-objective results of TPL-SW using NSUDTPSO

Set No.	W1	W2	Without device		With GUPFC	
			TPL (MW)	SW ($/h)	TPL (MW)	SW ($/h)
1	0.9	0.1	9.192	1077.026	8.95	1099.293
2	0.8	0.2	9.2165	1085.293	9.1029	1112.938
3	0.7	0.3	9.3246	1123.284	9.2323	1134.292
4	0.6	0.4	9.486	1167.839	9.4232	1178.385
5	0.5	0.5	9.606	1199.25	9.556	1188.865
6	0.4	0.6	9.6827	1219.293	9.7823	1212.321
7	0.3	0.7	9.7384	1228.212	9.8923	1217.713
8	0.2	0.8	9.8294	1239.121	10.1992	1228.322
9	0.1	0.9	9.986	1247.026	10.4323	1237.074

Table 6. Summary of multi-objective results of Vdev-SW using NSUDTPSO

Set No.	W1	W2	Without device		With GUPFC	
			Vdev (p.u.)	SW ($/h)	Vdev (p.u.)	SW ($/h)
1	0.9	0.1	0.21	1065.498	0.2013	1098.237
2	0.8	0.2	0.2232	1072.123	0.2124	1102.129
3	0.7	0.3	0.2421	1080.312	0.2344	1109.747
4	0.6	0.4	0.2612	1091.382	0.2492	1120.366
5	0.5	0.5	0.284	1097.501	0.2831	1133.977
6	0.4	0.6	0.3123	1101.123	0.3091	1162.255
7	0.3	0.7	0.3612	1105.354	0.3427	1203.773
8	0.2	0.8	0.4123	1107.928	0.4012	1236.12
9	0.1	0.9	0.451	1109.013	0.4499	1266.919

Table 7. Summary of multi-objective results of Vdev-TPL using NSUDTPSO

Set No.	W1	W2	Without device		With GUPFC	
			Vdev (p.u.)	TPL (MW)	Vdev (p.u.)	TPL (MW)
1	0.9	0.1	0.255	11.81	0.246	12.947
2	0.8	0.2	0.2764	11.2637	0.2673	12.2092
3	0.7	0.3	0.2984	11.0009	0.2831	11.5923
4	0.6	0.4	0.3628	10.7812	0.3231	11.0013
5	0.5	0.5	0.417	10.654	0.3771	10.5423
6	0.4	0.6	0.4672	10.5423	0.4721	10.4212
7	0.3	0.7	0.5172	10.4823	0.5213	10.3823
8	0.2	0.8	0.5787	10.4001	0.5819	10.3112
9	0.1	0.9	0.617	10.375	0.6312	10.269

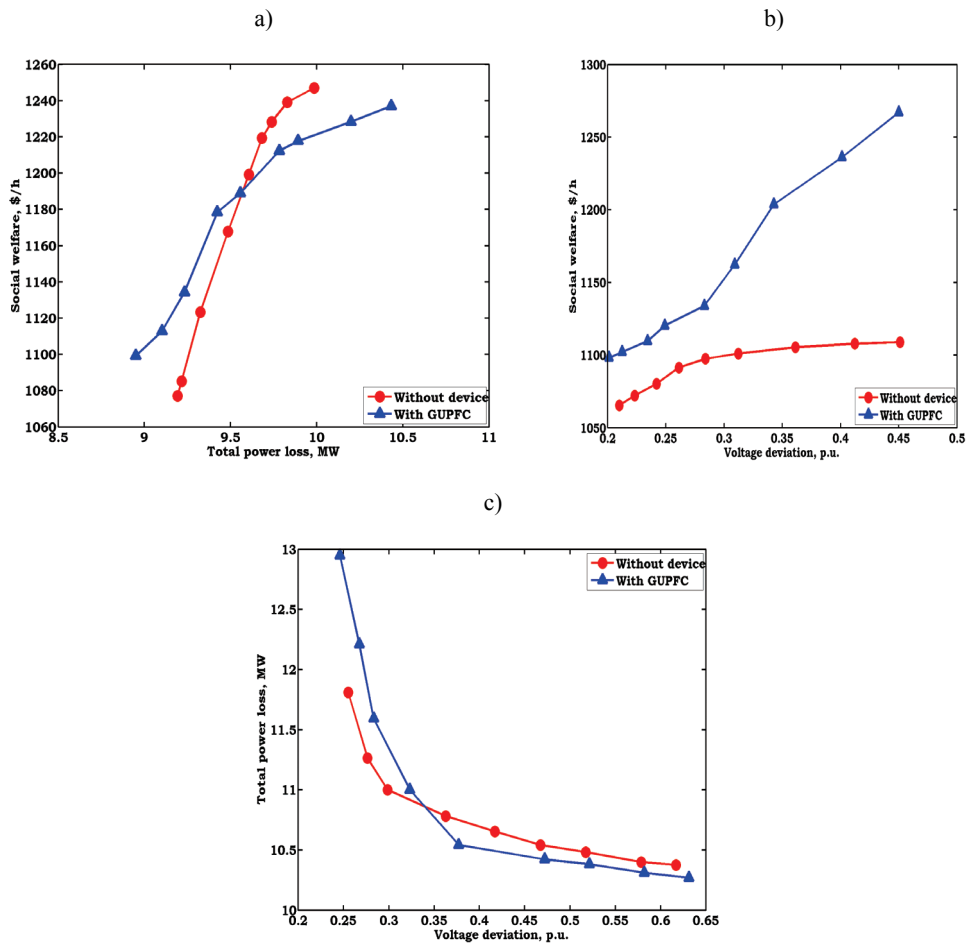a)   b)

c)

Fig. 5. Two dimensional Pareto solutions of case 4 with GUPFC: a) total power loss – social welfare combination, b) voltage deviation – social welfare, c) voltage deviation – total power loss

From these tables, it is observed that, better result has been obtained with GUPFC when compared to without device. It is observed that, based on weights assigned to the objectives, the respective function values were selected by the fuzzy decision making tool from the Pareto solutions. The corresponding two dimensional Pareto solutions when two objectives are considered is shown in Figure 5. From this figure, it is identified that, depending on the maximization or minimization of the objectives, the respective Pareto solutions are selected from the generated solutions.

The obtained result for case 5 is given in Table 8. From this table it is observed that, based on the weights assigned to objectives the fuzzy decision making tool selects the best values with GUPFC when compared to without device. The corresponding Pareto solution with GUPFC is shown in Figure 6. From this figure it is observed that the generated solutions confine the entire solution region because of the effectiveness of the proposed algorithm.

Table 8. Summary of multi-objective results of SW-TPL-Vdev using NSUDTPSO

| S. No	W1	W2	W3	Without device			GUPFC		
				SW ($/h)	TPL (MW)	Vdev (p.u.)	SW ($/h)	TPL (MW)	Vdev (p.u.)
1	0.1	0.1	0.8	983.607	10.606	0.237	1050.439	9.677	0.221
2	0.1	0.8	0.1	974.545	8.895	0.957	1064.325	8.706	0.36
3	0.8	0.1	0.1	1261.343	12.204	0.46	1341.396	10.875	0.815
4	0.5	0.4	0.1	1021.423	9.89	0.252	1274.731	9.796	0.461
5	0.5	0.1	0.4	1097.316	12.204	0.46	1259.141	11.791	0.287
6	0.4	0.5	0.1	974.545	8.895	0.957	1174.108	8.93	0.305
7	0.1	0.5	0.4	1012.351	9.87	0.259	1174.108	8.93	0.305
8	0.1	0.4	0.5	1162.115	9.12	0.313	1098.253	9.96	0.268
9	0.4	0.1	0.5	1097.316	11.791	0.287	1098.253	9.96	0.268
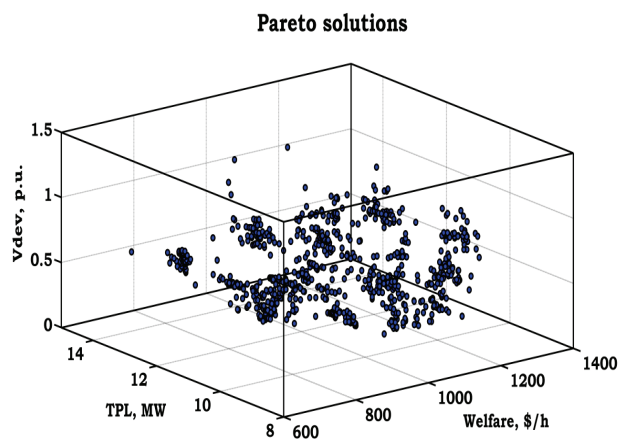
Fig. 6. Three dimensional Pareto solutions of case 5 with GUPFC

8. Conclusions

In this paper, we presented a power injection model for a GUPFC and determined the optimal location to enhance the system security by minimizing system severity function. A novel generation cost function was formulated using the multi-fuel costs of active and reactive power generation, along with the costs of shunt compensation and total transmission power losses. A novel optimization algorithm based on uniform distribution of control variables and two stage initialization processes has been presented to solve single objective OPF problems with social welfare, total power losses and voltage deviations as objective functions. The formulated OPF problem has been solved while satisfying system equality, in-equality, practical constraints and device limits. And also, the formulated multi-objective OPF problem to maximize the social welfare by optimally re-dispatching reactive power has been implemented using the proposed non-dominated sorting based UDTPSO algorithm. The obtained results are encouraging and the proposed methodology works independent of the nature of the problem and can be implemented to solve any size of the system for any number of objectives. The complete methodology has been tested on standard IEEE-30 bus system with supporting numerical and as well as graphical results.

Appendix

Table A1. Generator's active power cost coefficients

S. No	Gen. No	a	b	c	d	e	$P_G^{\min}$	$P_G^{\max}$
1	1	0.005	0.7	55	0.35	0.0032	50	140
		0.0075	1.05	82	0.254	0.00153	140	200
2	2	0.01	0.3	40	0.294	0.0029	20	55
		0.02	0.6	80	0.241	0.00165	55	80
3	5	0.0625	1	0	0	0	15	50
4	8	0.00834	3.25	0	0	0	10	35
5	11	0.025	3	0	0	0	10	30
6	13	0.025	3	0	0	0	12	40

Table A2. Generator's reactive power cost coefficients

S. No	Gen. No	ar	br	cr	dr	er	$Q_G^{\min}$	$Q_G^{\max}$
1	1	0.0005	0.07	5.5	0.035	0.00032	−20	100
		0.00075	0.105	8.2	0.0254	0.000153	100	200
2	2	0.001	0.03	4.0	0.0294	0.00029	−20	55
		0.002	0.06	8.0	0.0241	0.000165	55	100
3	5	0.00625	0.1	0	0	0	−15	80
4	8	0.000834	0.325	0	0	0	−15	60
5	11	0.0025	0.3	0	0	0	−10	50
6	13	0.0025	0.3	0	0	0	−15	60

References

 [1] Hasanpour S., Ghazi R., Javidi MH., *A new approach for cost allocation and reactive power pricing in a deregulated environment.* Electrical Engineering 91: 27-34 (2009).

 [2] Almeida KC., Senna F.S., *Optimal active-reactive power dispatch under competition via bilevel programming.* IEEE Transactions on Power Systems 26(4): 2345-2354 (2011).

 [3] Gomesa MH., Saraivab JT., *A market based active/reactive dispatch including transformer taps and reactor and capacitor banks using simulated annealing.* Electric Power Systems Research 79: 959-972 (2009).

 [4] Kundur P., *Power System Stability and Control.* McGraw-Hill, Inc., New York (1994).

 [5] Rabiee A., Shayanfar H., Amjady N., *Multi-objective clearing of reactive power market in deregulated power systems.* Applied Energy 86(9): 1555-1564 (2009).

 [6] *Operating Policy-10 on Interconnected Operation Services.* North American Electric Reliability Corporation (2000).

 [7] Xie K., Song YH., Stonham J., Yu E., Liu G., *Decomposition Model and Interior Point Methods for Optimal Spot Pricing of Electricity in Deregulated Environments.* IEEE Transactions on Power Systems 15(1): 39-50 (2000).

 [8] Verma KS., Gupta HO., *Impact on real and reactive power pricing in open power market using unified power flow controller.* IEEE Transactions on Power Systems 21(1): 365-371 (2006).

 [9] Verma KS., Singh SN., Gupta HO., *Optimal location of UPFC for congestion management.* Electrical Power Systems Research 58(2): 89-96 (2001).

[10] Verma KS., Singh SN., Gupta HO., *FACTS device location for enhancement of total transfer capability.* Proceedings of IEEE Power Engineering Society. Winter Meeting, Columbus 2: 522-527 (2001).

[11] Choi JY., Rim SH., Park JK., *Optimal real time pricing of real and reactive powers.* IEEE Transactions on Power Systems 13(4): 1226-1231 (1998).

[12] Lamont JW., Fu J., *Cost analysis of reactive power support.* IEEE Transactions Power Systems, 14(3): 890-896 (1999).

[13] Dai Y., Ni YX., Wen FS., Han ZX., *Analysis of reactive power pricing under deregulation.* Proceedings of IEEE Power Engineering Society, Summer Meeting, Seattle, pp. 2162-2167 (2000).

[14] Ranatunga R.A.S.K., Annakkage U.D., Kumble C.S., *Algorithms for incorporating reactive power into market dispatch.* Electrical Power Systems Research 65: 179-186 (2003).

[15] Ranatunga R.A.S.K., Annakkage U.D., Kumble C.S., *Implications of reactive power on nodal pricing and dispatch.* Proceedings of IEEE Power Engineering, Winter Meeting, pp. 885-890 (2000).

[16] Devaraj D., *Improved genetic algorithm for multi-objective reactive power dispatch problem.* European Transactions on Electrical Power 17(6): 569-581 (2007).

[17] Li Hongxin., Li Yinhong., Chen Jinfu., *Adaptive multiple evolutionary algorithms search for multi-objective optimal reactive power dispatch.* International Transactions on Electrical Energy Systems 24(6): 780-795 (2013).

[18] Taher Niknam., Mohammad Rasoul Narimani., Masoud Jabbari., *Dynamic optimal power flow using hybrid particle swarm optimization and simulated annealing.* International Transactions on Electrical Energy Systems 23(7): 975-1001 (2013).

[19] Hazra J, Sinha AK, *A multi-objective optimal power flow using particle swarm optimization.* European Transactions on Electrical Power 21(1): 1028-1045 (2011).

[20] Saravanan M., Mary Raja Slochanal S., Venkatesh P., Prince Stephen Abraham J., *Application of particle swarm optimization technique for optimal FACTS devices considering cost of installation and system loadability.* Electrical Power Systems Research 77: 276-283 (2007).

[21] Seyed M.H. Nabavi., Kamran Khafafi., Aidin Sakhavati., Saeid Nahi., *Optimal Location and Sizing of SSSC using Genetic Algorithm in Deregulated Power Market.* International Journal of Computer Applications 22(4): 37-41 (2011).

[22] Husam I. Shaheen., Ghamgeen I., Rashed S.J. Cheng., *Optimal location and parameter setting of UPFC for enhancing power system security based on differential evolution algorithm.* Electrical power and energy systems 33: 94-105 (2011).

[23] Y. Dai., X.D. Liu., Y.X. Ni., F.S. Wen., Z.H. Han., C.M. Shen., F.F. Wu., *A cost allocation method for reactive power service based in power flow tracing.* Electrical Power System Research 64: 59-65 (2003).

[24] C.Y. Chung., T.S. Chung., C.W. Yu., X.J. Lin., *Cost-based reactive power pricing with voltage security consideration in restructured power systems.* Electrical Power Systems Research 70: 85-91 (2004).

[25] Hao S., *A reactive power management proposal for transmission operators.* IEEE Transactions on Power Systems 18: 1374-1381 (2003).

[26] Naresh Babu, A.V., Ramana T., Sivanagaraju S., *Analysis of optimal power flow problem based on two stage initialization algorithm.* International Journal of Electrical Power and Energy Systems 55: 91-99 (2014).

[27] Niknam T., Narimani MR., Aghaei J., Azizipanah-Abarghooee R., *Improved particle swarm optimization for multi-objective optimal power flow considering the cost, loss, emission and voltage stability index.* IET Generation, Transmission & Distribution 6(6): 515-527 (2012).

[28] Kennedy J., Eberhart R., *Particle Swarm Optimization.* IEEE International conference on Neural Networks 4: 1942-1948 (1995).

[29] Dhillon JS., Parti SC, Kothari DP., *Stochastic economic emission load dispatch.* Electric Power Systems Research 26: 179-186 (1993).

[30] Vaisakh K., Praveena P., Rama Mohana Rao S., Kala Meah., *Solving dynamic economic dispatch problem with security constraints using bacterial foraging PSO-DE algorithm.* Electrical Power and Energy Systems 39: 56-67 (2012).

[31] Kalyanmoy Deb., Samir Agarwal., Amrit Pratap., Meyarivan T., *A Fast Elitist Non-Dominated Sorting Genetic Algorithm for Multi-Objective Optimization: NSGA-II.* Kanpur Genetic Algorithms Laboratory, IIT Kanpur.

[32] Abido MA., *Optimal power flow using Tabu search algorithm.* Electric Power Components and Systems 30: 469-483 (2002).

[33] Alsac O., Stott B., *Optimal Load Flow with steady state security.* IEEE PES summer meeting and EHV/UHV conference, pp.745-751 (1973).

[34] Arul R., Ravi G., Velsami S., *Non-convex economic dispatch with heuristic load patterns, valve point loading effect, prohibited operating zones, ramp-rate limits, and spinning reserve constraints using harmony search algorithm.* Electrical Engineering 95: 53-61 (2013).

[35] Chanda Sandip., Abhinandan De., *A multi-objective solution algorithm for optimum utilization of smart Grid infrastructure towards social welfare.* Electrical Power and Energy Systems 58: 307-318 (2014).